Journal of Computational Science 73 (2023) 102137

Contents lists available at ScienceDirect

Journal of Computational Science

journal homepage: www.elsevier.com/locate/jocs

Why does history surprise us?

Janusz A. Hołyst

Faculty of Physics, Warsaw University of Technology, Koszykowa 75, Warsaw, 00-662, Poland

ARTICLE INFO

Keywords:
Discontinuous phase transition
Social impact
Communities
Structural balance
Tipping points
Fold catastrophe

ABSTRACT

The Russian military aggression against Ukraine in February 2022 unveiled the illusory nature of our faith in the stability of the global political system. This belief was largely rooted in our short-term observations and naive expectations that political structures and social relationships were fixed points in the evolution of history. However, the reality is that we cannot assume the socio-political order we know to be the sole possible state, nor should we expect the transition to new solutions to occur smoothly. This study presents three agent-based models demonstrating how changes in socio-political structures can exhibit a discontinuous nature. These models include a social impact model with a strong leader, a model of interactions among competing social groups, and a model of structural balance dynamics. The discontinuous changes observed stem from the multistability of multiagent models, and the resulting transitions are both irreversible and exhibit hysteresis behaviour. All the transitions considered correspond to tipping points and the critical parameter values calculated through analytical approaches agree with the results of agent-based numerical simulations. The outcomes of these models exhibit qualitative agreement with historical data, particularly concerning the causes of the First World War and Adolf Hitler's ascent to absolute power in Germany, while also complementing observed variations in connection density within echo chambers formed by conservative and liberal communities in U.S.

1. Introduction

Theoretical physics, coupled with computer simulations, has developed universal tools that enable the comprehension of objects as disparate as elementary particles, crystals, liquids, stars, and galaxies. Some of these tools, in conjunction with insights from psychology, sociology, and history, also facilitate the examination of social phenomena. Research in this realm falls under the purview of fields known as sociodynamics [1–3] or sociophysics [4–11]. Sociophysics is closely aligned with computational social science [12], which embodies a data-driven approach to studying social phenomena [13,14]. However, it encompasses not only models of opinion change [15,16] but also interdisciplinary enquiries such as pedestrian dynamics [17], traffic flows [18,19], urban dynamics [20], the emergence of cooperation [21], mortality [22], and the science of science [23].

Most foreign policy is formulated on the basis of scenarios that assume a high degree of continuity, inertia, and incremental changes within international systems. However, the Russian military aggression against Ukraine in February 2022 vividly demonstrated the illusory nature of our confidence in the stability of the global political system. This conviction largely emanated from the limited timeframe of our observations and our naive expectations that the prevailing political structures and social relationships were fixed points in the trajectory of history's evolution. Nevertheless, there exists no compelling reason to posit that the socio-political order familiar to us constitutes the exclusive feasible solution, or that the transition to novel solutions must necessarily unfold along a smooth trajectory. Indeed, as seen in political scenarios, discontinuous changes can also transpire [24–26].

The primary objectives of this paper are threefold: (i) to present a concise overview of agent-based models wherein shifts in socio-political structures exhibit a discontinuous nature; (ii) to illustrate that the behaviour of these models arises from shared topological characteristics of system trajectories; and (iii) to demonstrate that these discussed models qualitatively capture well-documented historical transitions or data related to selected social groups forming echo chambers.

Our focus will be directed toward specific systems that encapsulate what is commonly referred to as *tipping points* within *nonlinear* social opinion dynamics, which emerge due to the existence of multiple equilibria. Upon reaching a tipping point (a threshold level), the trajectory of the system transforms into a runaway process [15,27–29], and the tipping point prevents a straightforward return to an earlier equilibrium. Consequently, these systems manifest hysteresis trajectories.

In particular, we undertake a review and comparative analysis of the following models:

E-mail address: janusz.holyst@pw.edu.pl.

https://doi.org/10.1016/j.jocs.2023.102137
Received 24 December 2022; Received in revised form 22 August 2023; Accepted 25 August 2023
Available online 14 September 2023

1. The model of a strong leader is grounded in the theory of social impact and demonstrates that an agent possessing a significantly strong influence (referred to as the leader's "charisma") can catalyze the formation of a group or party around them. Crossing a certain social strength threshold for such a leader triggers a discontinuous surge in the number of his followers [4,30,31].
2. A similar step-like alteration in the number of adherents to a given opinion may arise during the collision of two initially isolated social groups. Elevating the strength of interactions between these groups beyond a critical threshold results in a sudden alteration of opinions within one of the groups. Remarkably, a smaller community might exhibit greater stability if its internal connections are denser than the links within the larger, more sparsely connected community.
3. Interactions involving three agents, described as *a friend of my friend* and *an enemy of my enemy* are *my friends*, along with *an enemy of my friend* and *a friend of my enemy* are *my enemies*, can lead to a phenomenon known as *structural balance* [32–35]. This balance, contingent on model parameters and system history, extends beyond common friendship (paradise state) to encompass polarized states — the division of a community into subgroups holding opposing opinions. In the presence of noise, the system undergoes a discontinuous and irreversible transition to a disordered state [36] when the noise level surpasses a critical threshold.

The dynamics of all three models belong to a broad class of *complex contested contagion* [37], wherein changes to nodes or link attributes within corresponding social networks can occur when a *collective influence* exerted by neighbouring agents (including a countervailing impact of two conflicting opinions) surpasses specific thresholds. The incorporation of noise endows activation thresholds with a fuzzy nature.

Tipping points are present within all the models under consideration. They can be approached through adjustments to relevant model parameters, such as the strength of a social leader, the number of cross-links connecting diverse communities, or the noise intensity in the agent system striving for structural balance. Effects of noise can sometimes be counterintuitive, as a range of noise levels can lead to states of reduced entropy corresponding to social homogenization for groups with leaders or pairs of interacting communities.

Movies visualizing the aforementioned multi-agent dynamics can be accessed at https://www.youtube.com/watch?v=q8uPiFaUKOg&t=17501s, and corresponding programs are available at https://drive.google.com/drive/folders/1txUwC3jbSpazqokytqhrN5kKGl_ldFxU?usp=sharing.

Fig. 1. Mahatma Gandhi and his supporters during the *Salt March* from Sabarmati Ashram in Ahmedabad to the Arabian Sea at Dandi, India (1930). The march was part of his nonviolent resistance campaign that contributed to India's independence.
Source: Credit: Keystone/Getty Images.

Fig. 2. Adolf Hitler, Chancellor of Germany, with his supporters in Nuremberg (1933). Hitler's adept oratory skills played a significant role in transforming a democracy into a tyranny.
Source: Credit: Hulton Archive/Getty Images.

2. When a strong leader seizes absolute power

Leaders in politics are undeniably pivotal figures, although their roles may not invariably be positive. Prominent political leaders like Mahatma Gandhi (see Fig. 1) and Lech Wałęsa have made substantial contributions to their nations. Conversely, there have been instances of leaders with profoundly negative impacts, exemplified by Adolf Hitler (see Fig. 2), who was central to the perpetration of the Holocaust. It is noteworthy that many leaders established their political influence by initiating movements with a small group of followers, which grew over time to attain majority status through *democratic* decisions of a nation [26].

The phenomenon of a strong leader is clearly exemplified through a well-suited application of social impact theory (SIT), formulated by social psychologist Bibb Latané in the 1980s [38,39]. In SIT, individuals can be sources or targets of social influence—termed social impact. SIT is a natural foundation for agent-based modelling when depicting agents with varying social strengths. In the SIT framework, an individual agent has the capacity to alter his opinion due to the cumulative impact of other agents, particularly when the influence from those who support the agent's existing opinion is outweighed by the persuasive power of agents holding an opposing viewpoint [38,40]. In this way, the SIT framework falls within a wider category of intricate contested contagion models [37]. This theory finds application in various contexts, for instance, it helps in understanding the role of norms in shaping human behaviour [41], exploring self-organization within e-gaming communities [42], and providing insights into interactions on social media platforms [43].

In its simplest rendition, a SIT model comprises N agents (members of a social group), each holding one of two opposing opinions, denoted as $\sigma_i(t) = \pm 1$, where $i = 1, 2, 3, \dots, N$ [40]. Such a binary opinion representation is apt when addressing highly contentious issues [38,39]. Agents are situated within a social space, where each pair of individuals (i, j) is assigned a social distance d_{ij} and agents exert influence on one another, with this influence diminishing as the distance increases. This influence leads to opinion changes over time, reminiscent of the kinetic Ising model with $s = 1/2$ [40]. Notably different from spin systems, individuals possess varying levels of impact power, represented by the parameter $s_i > 0$, signifying their *social strength* of influence and the impact exerted at the agent i can be written as follows [30,40]

$$I_i = -s_i \beta - \sum_{j=1, j \neq i}^{N} \frac{s_j \sigma_i \sigma_j}{g(d_{ij})} \tag{1}$$

where parameter $\beta > 0$ characterizes self-support (agents' ability to sustain own opinions) and the function $g(d_{ij})$ delineates the impact of social influence's decline with increasing social distances d_{ij}.

Changes in opinions are guided by the collective social impact $I_i(t)$ as follows:

$$\sigma_i(t+1) = \sigma_i(t)\,\mathrm{sign}[-I_i(t)]. \tag{2}$$

Eq. (2) means that the agent i maintains his opinion only when a negative impact $I_i(t)$ is perceived at a given moment. Let us emphasize that the discrete-time dynamics of this model are justified, as our opinions do not undergo continuous changes, aligning with the binary representation of agent opinions. Eq. (2) represents completely deterministic dynamics but it can be extended to the stochastic case either by adding to the rhs of Eq. (1) a stochastic variable or using a Glauber approach as follows [30,44]

$$\sigma_i(t+1) = \begin{cases} \sigma_i(t), & \text{with probability } P_i; \\ -\sigma_i(t), & \text{with probability } 1 - P_i. \end{cases} \tag{3}$$

where:

$$P_i = \frac{\exp(-I_i/T)}{\exp(-I_i/T) + \exp(I_i/T)} \tag{4}$$

Here the parameter $T > 0$ is a measure of social noise level describing the degree of system randomness and it corresponds to the temperature or the noise level in physical processes. This noise encompasses various random influences that evade deterministic description within this model's framework. These influences can originate from both *external* sources like mass media [45,46] or chance interactions with agents beyond the considered group, as well as *internal* sources like personal reflections/meditations or irrational spontaneous/unconscious decisions [47,48]. When $T \to 0_+$ then Eq. (3) reduces to Eq. (2).

It is crucial to underscore that the social impact model [38,39] elucidates opinion changes and does not distinguish between peaceful and violent societal processes. This implies that opposing opinions represented by variables $\sigma_i(t)$ can correspond to such diverse attributes as fashion preferences or conflicting political sentiments.

Fig. 3 illustrates the dynamics of social impact for $N = 576$ agents positioned on a square lattice with boundary conditions that do not include agents beyond this square. Blue and red circles depict opinions $\sigma_i(t)$, and black bars represent agent strengths s_i. Social distance d_{ij} is computed using Euclidean metrics, and the decline of social influence follows as $1/g(d_{ij}) = d_{ij}^{-\alpha}$. Results are presented here for the exponent $\alpha = 4$, yet it has been demonstrated [30] that the principal characteristics of this model hold true for $\alpha = 1, 2, 3$ as well. Furthermore, instead of considering agents within a two-dimensional Euclidean geometry (enabling a more accessible visualization of changes in agents' opinions) where mutual interactions depend on distances d_{ij}, a more general system of agents can be explored [44], incorporating an immediacy matrix m_{ij}. The matrix serves as a counterpart to the function $1/g(d_{ij})$, with diagonal terms m_{ii} signifying self-support effects. Special instances of immediacy matrix m_{ij} can also be employed to mirror a topology of a social group through a suitable complex network.

Panel 3(a) depicts the initial conditions where strengths and opinions have been randomly assigned. Panel 3(b) displays the configuration at time moment $t = 9$ where the dynamics adhere to Eqs. (2) and (1) without noise was applied. Domains of red and blue opinions have emerged, and the ratio N_r/N_b of the number of red to blue representatives in this panel stands at 344/232. The blue opinion of the minority has persevered in four large clusters near the system boundary, along with a small central cluster comprising two agents with high social strengths (larger black bars). This configuration is a fixed point of the dynamics, with the pattern remaining unchanged in subsequent time steps. Panel 3(c) depicts the opinion pattern at time moment $t = 43$ with noise of strength $T = 8$ as defined in Eq. (3). Some blue domains have contracted or vanished, altering the ratio N_r/N_b to 424/152. Panel 3(d) showcases the configuration at $t = 234$. The noise aids the further expansion of the red majority, resulting in the ratio $N_r/N_b = 437/139$. This process is even more pronounced in panel 3(e), where the noise intensity is heightened to $T = 16$, and the snapshot is taken at $t = 813$. The blue opinion has nearly vanished, leaving only 16 blue agents (indeed, most of these blue "dissidents" are fleeting fluctuations with a lifespan of $\delta t = 1$).

We observe that the noise has eliminated one of the opinions. This occurs because the multi-domain patterns seen in panels 3(b–d) are metastable configurations, and a slight noise perturbation shifts the system toward the "ground state", where all agents are red (with slightly different initial conditions, the "ground state" with all blue agents could be reached). Such a state is robust, and in a large system, it is highly improbable for the system trajectory to substantially deviate from this "ground state" due to fluctuations. However, the scenario changes when the noise intensity is significantly greater, as illustrated in panel 3(f) corresponding to the noise intensity $T = 30$ and the time moment $t = 1112$. Such intense noise disrupts most opinion clusters, resulting in nearly equal numbers of red and blue representatives (the ratio N_r/N_b is 283/293 in this panel).

Now let us consider a scenario where all agents within the group possess the same individual strength, denoted as $S_i = 1$, except for one individual who will be referred to as the "leader". The leader holds significant influence, with his strength marked as $S_L \gg 1$. To facilitate analytical calculations, the leader is positioned at the centre of a circular social group with a radius of R (as depicted in Fig. 4). As the leader's strength S_L increases (illustrated in panels (a) and (b) of Fig. 4), the number of his supporters also grows, resulting in the expansion of his faction. This progression is straightforward.

However, what is far from straightforward is the observation that, upon surpassing a certain threshold, a remarkable phenomenon occurs: suddenly, there is no longer any opposition to the leader's influence (as seen in panel (c) of Fig. 4). The presence of the opposing "blue" phase disappears, leaving only advocates of a single opinion. It is important to emphasize that this substantial shift in the number of followers supporting the leader happens with only a slight increase in the leader's strength, transitioning from $S_L = 237$ (panel (b) of Fig. 4) to $S_L = 238$ (panel (c) of Fig. 4). The discontinuous change results from crossing a separatrix curve, often referred to as a tipping point [15]. This curve divides distinct domains of attraction within the underlying dynamical system, and you can find a more detailed discussion in the section below Eq. (5).

A similar transition towards the leader's party dominance can be achieved even with a less potent leader by introducing noise into the system (refer to Eq. (3)). The effects of this noise are visible in panels (d) and (e) of Fig. 4. In these simulations, the leader's strength is set at $S_L = 150$ (still significantly higher than the strength $S_i = 1$ of the other agents), and a minor noise level is present.

In panel (d), the results after 9 time steps show a well-organized red party at the centre of the community, surrounded by a chaotic mixture of blue and red at the periphery. Shifting to panel (e), representing the outcome after 10 time steps, the previously disordered mixture at the periphery transforms into a red phase consisting mainly of the leader's supporters, with only a few remaining blue dissidents.

Analytical results for the critical leader strength S_{Lc}, marking the transition to dictatorship, are available in Ref. [30]; see also Refs. [4,31,44]. By disregarding self-support effects (setting $\beta = 0$ in Eq. (1)), and assuming that social interactions in Eq. (1) decay with distance d_{ij} as $1/g(d_{ij}) = 1/d_{ij}$, we can approximate the radius a of the leader's party as:

$$a \approx \frac{1}{8}\left(\pi R - \sqrt{\pi^2 R^2 - 8S_L}\right) \tag{5}$$

Results for other values of exponents describing the decays of social interactions can be found in [30]. When $S_L > S_{Lc} = \pi^2 R^2/8$, Eq. (5) lacks real solutions. Consequently, the coexistence of a leader-centred party and an opposing ring is no longer feasible. As the leader's strength

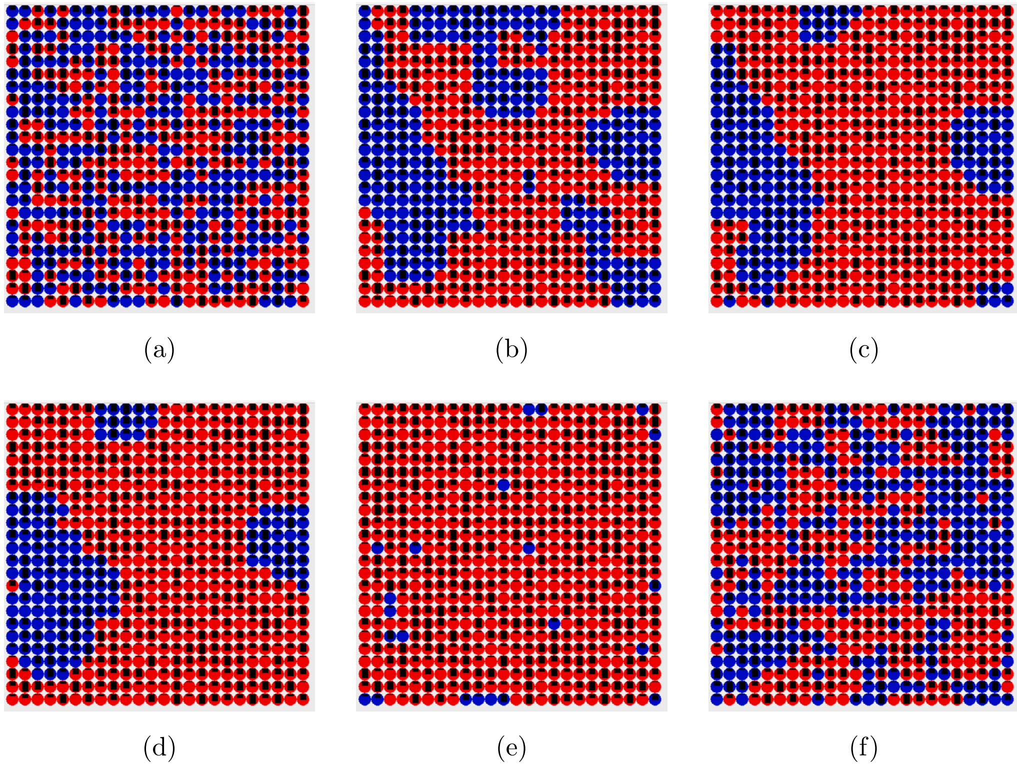

Fig. 3. Changes in opinions within a social group governed by the dynamics of social impact theory. Red and blue circles correspond to two distinct opinions, while black bars indicate various agents' strengths. (a) - random initial conditions; (b) - configuration at time moment $t = 9$ - the blue minority has persisted in a few clusters (fixed point of noise-free dynamics); (c), (d), (e), (f) - the evolution of the system under the influence of noise measured by the parameter T. Opinions $\sigma_i(t)$ are updated simultaneously (synchronous dynamics) in discrete time steps according to the rule given by Eq. (3).

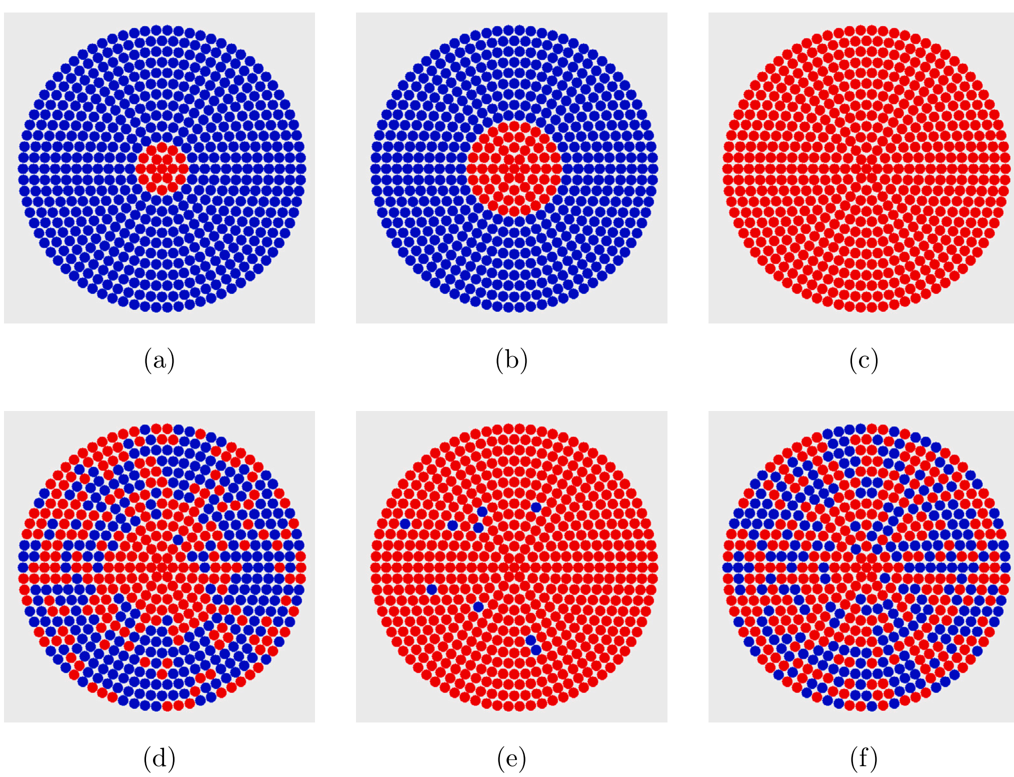

Fig. 4. Opinion evolution in a social group with 600 agents for the SIT dynamics (see Eq. (1) and (2)) for various strengths S_L of the leader placed in the centre of the group. Panel (a): $S_L = 150$, panel (b): $S_L = 237$, panel (c): $S_L = 238$. Panels (d) and (e): $S_L = 150$ and a small noise added to the dynamics, (d) corresponds to the time moment $t = 9$ and (e) corresponds to the time moment $t = 10$ (time is measured in macrosteps units when each agent is updated once). Panel (f) describes the case $S_L = 150$ and large noise intensity.

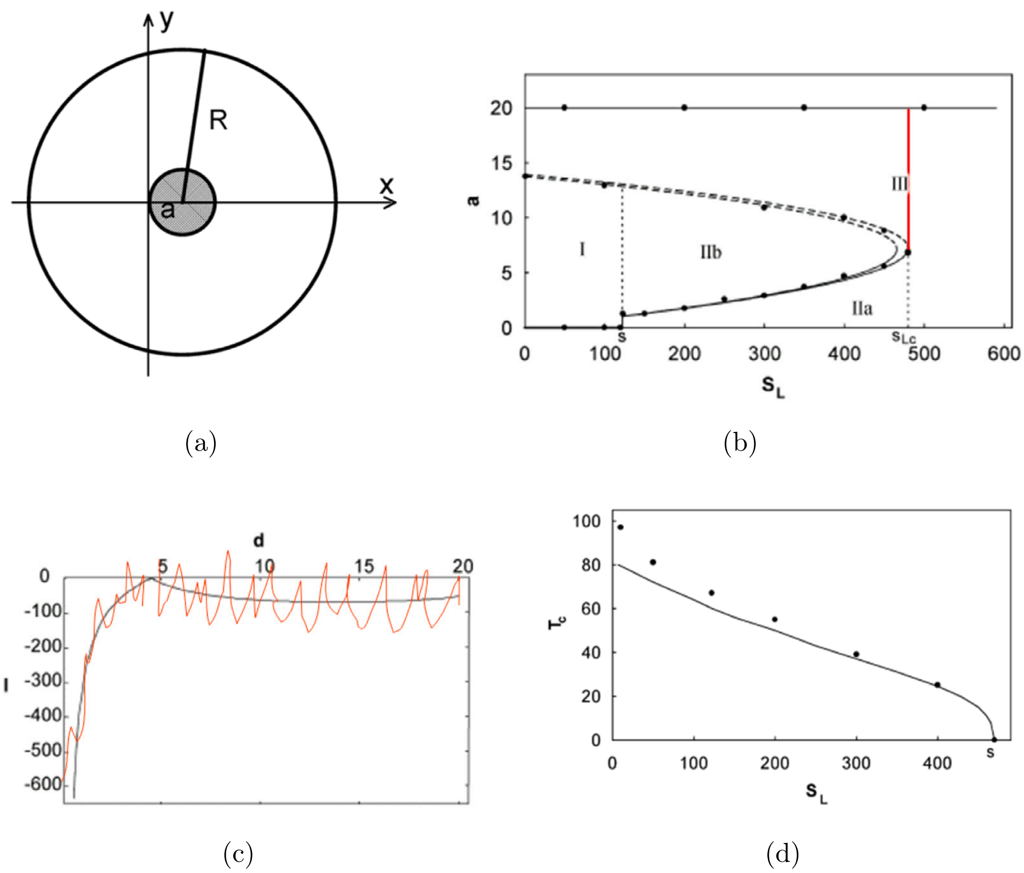

Fig. 5. Discontinuous phase transition in the model of a strong leader. (a) Circular cluster with a radius of a are leader followers surrounding a strong leader positioned at the centre of a social group of a radius R. (b) Phase diagram of the model, illustrating the relationship between the radius a of the leader's followers cluster and the leader's strength S_L. When $S_L < S_{Lmin}$, the leader cannot stand alone with his opinion (Region I), whereas when $S_L > S_{Lc}$, all agents align with the leader's party. Regions IIa and IIb denote the coexistence of the leader's party and the opposition. Full black line — analytical solution, dots — results of numerical simulations. Dashed lines stem from the presence of a separatrix between different attraction domains, with the red line denoting an irreversible and discontinuous transition at the tipping point. (c) Black line — deterministic part of social impact $I(d)$ vs. a distance d from the leader. The red curve — effect of noise. (d) Critical value of social noise T_c required to dismantle the leader's opposition versus the strength of the leader S_L. The line — analytical calculations, points — simulation results.
Source: Adapted from [31].

S_L exceeds S_{Lc}, the radius a of the leader's party jumps discontinuously from $\pi R/8$ to R, and the number of leader followers undergoes a sudden increase from $(\pi/8)^2 N \approx 0.154N$ to N. Importantly, this change is not only discontinuous but also irreversible and corresponds to the system tipping point. Even if the leader's authority S_L drops below S_{Lc}, the number of followers remains constant due to the absence of seeds for an alternative opinion.

The amplifying effect of slight social noise on the leader's effective power becomes apparent when examining social impact as a function of distance from the charismatic leader (panel (c) of Fig. 5). In this representation, red fluctuations signify noise, and some agents experience a positive impact, prompting opinion shifts. Notably, members of the leader's party, deeply ingrained in their allegiance, remain unswayed by noise. Conversely, those in the opposition are less steadfast, rendering them susceptible to opinion changes due to the interplay of the deterministic part of social impact and noise. Essentially, noise allows a potent political centre to attract more new supporters than those departing, potentially transforming the system from a two-domain state (leader party and opposition) to a single-domain state. This transition hinges on the leader's potency. A sufficiently powerful leader can establish a dictatorship sans noise. Even a weak leader can seize power through societal disorientation.

Therefore, the strategy to secure absolute power involves not only establishing a strong and influential political centre but also introducing processes that sow confusion in society and increase the level of social noise responsible for irrational behaviour.

The results also mean that a moderate noise can *order* the system by moving it from a state with two domains (leader party and opposition) to a state with one domain. Both states correspond to local equilibria of this system, and for a certain range of parameters, they coexist in the system's phase diagram (see Fig. 5b). However, the state of single-party domination is more stable and can also exist when the two domains' state disappears. A similar *ordering* effect of a small noise was observed in a driven model of pedestrians moving in a passage and named *freezing by heating* [49]. The pattern observed in the panel (d) of Fig. 5 resembles the phase diagram of some superconductive materials.

The data points in panels (b) and (d) of Fig. 5 correspond to numerical simulations, while the lines represent analytical results. For comprehensive information, refer to [4,30,31,44]. Certainly, the aforementioned model is intentionally simplistic, as real social groups do not conform to circular shapes. Nonetheless, it qualitatively encapsulates the dynamics witnessed in Germany during 1933, when Adolf Hitler and his party ascended to power amidst the politically unsettled Weimar Republic. Hitler adeptly formed a potent political faction and utilized various propaganda strategies to disorient society on a massive scale [26].

Illustrating the irrevocable polarization provoked by a forceful leader, we observe this phenomenon through successive parliamentary elections in Germany from 1918 to 1938 [50–53]. The increasing influence of Adolf Hitler is vividly depicted in Fig. 6, showcasing the percentage of seats secured by the German Nazi Parties – the National Socialist German Workers' Party (NSDAP) and its predecessors

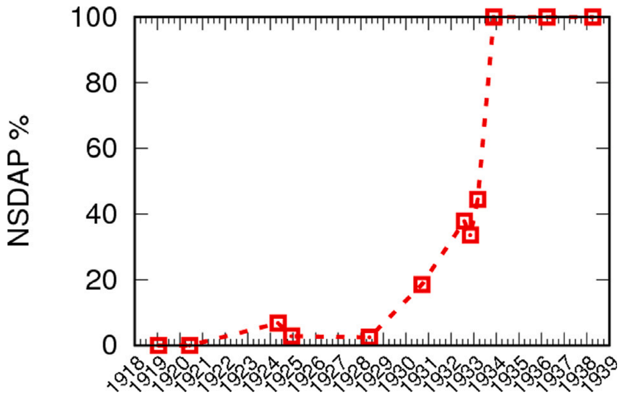

Fig. 6. The rapid rise of NSDAP election shares in the Weimar Republic during the period 1930–1932 quantitatively aligns with the outcomes of the strong leader model (compare with Fig. 5c).
Source: Historical data sources: [50–53].

– in federal election outcomes (1924–1938). Support for the NSDAP experienced a dramatic surge from 1928 to 1933. On March 5, 1933, the NSDAP garnered 44.5% of Reichstag mandates, enabling Hitler and his associates to seize absolute power in the Weimar Republic. Within months, Germany underwent a transformation from a parliamentary republic to a one-party totalitarian police state, where all opposition parties were proscribed.

In subsequent parliamentary elections, such as the one on November 12, 1933, only representatives of the NSDAP and its supporters were elected. In the 1936 and 1938 elections, a single-question referendum format asked whether voters approved a sole list of Nazi and pro-Nazi guest candidates, resulting in the NSDAP receiving over 97% of the votes and all parliamentary seats. Notably, the support for Adolf Hitler and the NSDAP, as depicted in Fig. 6, increased in a discontinuous manner, akin to the growth of strong leader supporters shown in Fig. 5(c) for the social impact model. Economic and social factors contributing to Hitler's rise from 1928 to 1933 are outside the scope of this paper and they are elucidated in works such as [26].

The swift ascent of NSDAP popularity before 1933 could have potentially served as an indicator for the impending transition toward complete societal polarization. Nevertheless, the model lacks the capacity to predict the outbreak of widespread violence in Germany under NSDAP rule. The onset of violence requires a separate model that comprehends the intricacies of the political changes under consideration, along with the dynamics between opposing social groups.

3. Discontinuous transitions in opinions of weakly coupled social groups

Social networks often exhibit a modular topology, composed of communities [54–56]. Consider two social groups, denoted as A and B (two distinct communities), with a loose connection. In other words, the density of "inter-links" connecting agents from different groups is significantly lower than that of "intra-links" binding agents within the same group. This implies weak interaction or influence between the groups. Similar to the SIT models discussed earlier, each agent a holds an opinion represented as $\sigma_a = \pm 1$. Notably, all agents share identical social strengths, ensuring symmetrical interactions. The dynamics of these opinions adhere to the Ising Hamiltonian:

$$H = H_A + H_B + H_{AB} \tag{6}$$

Here, H_A (H_B) characterizes interactions among agents iA (iB) within group A (B), while H_{AB} captures interactions between agents from distinct groups. The Hamiltonians have the following forms [57, 58]:

$$H_A = -\sum_{iA \neq jA} J_{iA,jA}\sigma_{iA}\sigma_{jA} \tag{7}$$

$$H_B = -\sum_{iB \neq jB} J_{iB,jB}\sigma_{iB}\sigma_{jB} \tag{8}$$

$$H_{AB} = -\sum_{iA,jB} J_{iA,jB}\sigma_{iA}\sigma_{jB} \tag{9}$$

Here, $J_{x,y} = J_{y,x}$ represents interaction constants for the mutual influence between agents labelled as x and y. These constants are either zero (indicating no connection between agents) or positive, signifying an agent's endeavour to persuade another agent to adopt his opinion (and vice versa). Our assumption about weak group interactions holds when only a few inter-group interaction constants $J_{iA,jB}$ are nonzero.

Let us represent the groups with graphs as shown in Fig. 7. The simulations presented here were conducted on synthetic scale-free networks; however, comparable outcomes for other topologies can be found in [58]. Group A comprises 50 agents and is termed the "yellow group" due to its 205 yellow intra-links. The larger group, B, consists of 80 agents and is called the "green group" with 185 green intra-links. Opinions σ_a in both groups are depicted by blue circles ($\sigma_a = -1$) or red circles ($\sigma_a = 1$). Given the loose connection between the groups, one can set initial conditions where members of group A lean toward the red opinion, while members of the group B favour the blue opinion. This configuration is depicted in the left panel of Fig. 7.

Our model employs Glauber dynamics [57,58], wherein individual opinion changes are influenced by a local field stemming from the nearest neighbours' opinions of a given agent. The probabilities of such changes depend on the system temperature T, which signifies the noise intensity level within the system. When the number of inter-links remains small and the temperature T is low, opinion fluctuations in both groups remain minor. Consequently, the mean opinion is near $+1$ for the yellow group and approximately -1 for the green group. This is evident in the left segment of the bottom panel in Fig. 7.

Subsequently, as time progresses, we increment the number of inter-links between the two groups. While these inter-links are randomly introduced and could slightly alter the degree distribution and clustering coefficients in both networks, their primary effect is to expose agents to opposing opinions from the other group. When this inter-link count crosses a critical threshold, the group interactions can no longer be negligible. Consequently, one of the groups is expected to shift its opinion due to the opposing influence from the other group. Naively, one might anticipate that the smaller group A would undergo such a change. However, the right panel of Fig. 7 demonstrates that group A maintains its red opinion, and it is the larger group B that transitions from the blue to the red opinion. This transition is also evident in the right segment of the bottom panel of Fig. 7, where the green curve exhibits a sudden upward shift. In fact, the time series displays a kink, signifying the rapid transition of the mean opinion within the entire green group.

Why was the smaller yellow group stronger, i.e., more resistant to changes in its opinion? The secret lies in the higher number of intra-links connecting members of this group. The group could withstand the opinion influence from the larger group due to denser internal connections within the smaller group, which effectively stabilized the opinions of its members. This underscores a clear message to politicians: to ensure resilience, construct a dense network of connections within your party and prevent its fragmentation when facing opposition from another party. Notably, leveraging methods from statistical physics [57,58], it becomes possible not only to identify the group likely to undergo opinion change but also to estimate the required number of inter-links for such an alteration. These calculations rely on the knowledge of both groups' structures, requiring comprehensive information about agents' connections.

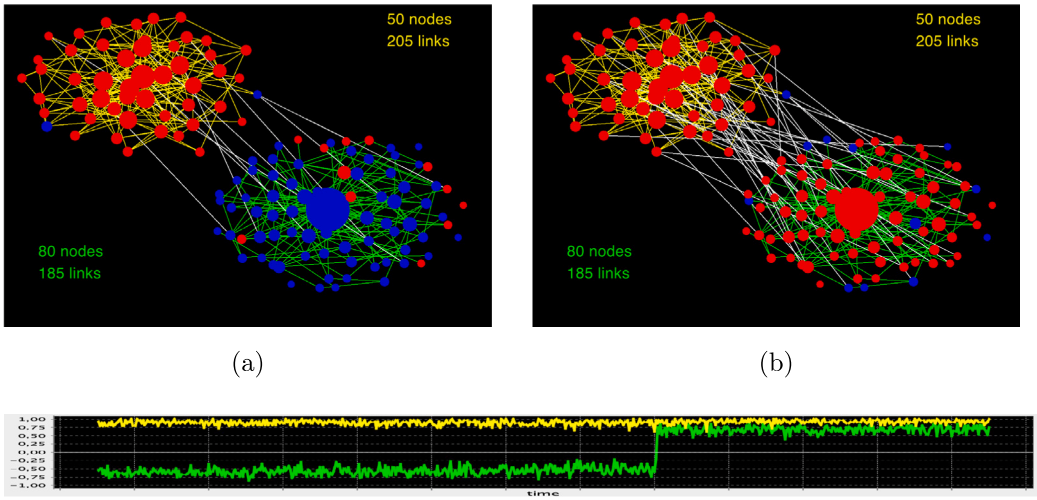

(c)

Fig. 7. Opinion changes in weakly connected groups with Ising-Glauber dynamics. The group A linked by yellow connections comprises 50 agents and 205 links, while the group B linked by green connections includes 80 agents and 185 links. The red and blue circles denote $+1$ or -1 opinions, respectively. Upper left panel: the initial configuration displays sporadic inter-links connecting both groups, with distinct opinions within each group. Upper right panel: with more inter-links, opinions in both groups align, causing the blue opinion in the larger group to vanish. Bottom panel: time series illustrating mean opinions in both groups. The green line depicts the opinion within the group linked by green connections, while the yellow line represents the opinion in the group linked by yellow connections. The sharp shift in the opinion of the larger (green) group is attributed to the increasing influence of the smaller (yellow) group, facilitated by the growing number of inter-links.

Can an external observer forecast the outcome of the competition between these groups without intricate details about their internal structures? The answer is "yes", as the susceptibility of a group to external influence (i.e., through inter-links connecting it with a group holding opposite opinions) is proportional to the variance of *fluctuations* of the mean opinion within the group *prior* to introducing external influence. This deduction stems from the so-called linear response theory [59]. The left segment of the bottom panel of Fig. 7 illustrates that fluctuations in the yellow group were considerably lower than those in the green group. Therefore, even without insight into the topology, it is feasible to predict interaction outcomes between the groups solely by observing opinion fluctuations within both groups.

Let us note the similarities between the model of the strong leader discussed in the previous section within the framework of SIT and the model of weakly coupled communities. In this context, the smaller yet denser connected community A assumes the role of a strong leader. If the influence of this community on community B becomes too strong, there is no room for the simultaneous presence of two opinions within this system. This is akin to the model of the strong leader, where the opposition had no space to exist when the leader's influence was too pronounced. The system exhibits multistability. The state of having two opinions represents a local equilibrium within the system, existing only within a certain parameter range. However, a more stable state involves a single opinion. At the tipping point, the phase characterized by differing opinions in both communities loses its stability, and only a state of social homogenization prevails.

While the dynamics of the considered Ising model are aligned with the broad complex contested contagion category [37], the observed discontinuous phase transition distinguishes itself from transitions witnessed in the threshold model [37] on one-dimensional rings with random long-ties. In the threshold model [37], efficient opinion propagation can occur through targeted cross-links forming *broad bridges* or *hybrid contagions*, where certain nodes with lower threshold values act as *early adopters*. In contrast, our model introduces cross-links randomly and lacks thresholds in its dynamics. Nonetheless, the larger group adopts the opinion of the smaller group for two reasons: (i) the larger group contains numerous nodes with low connection degrees to agents within their group, making a cross-link from the smaller group a potent influence biased toward the opinion of the latter group; (ii) Ising - Glauber dynamics is not deterministic, with thermal noise prompting spontaneous opinion flips. Such fluctuations are more prevalent in the larger group (refer to panel (c) of Fig. 7), given the smaller mean node degree in this group. Consequently, nodes within this larger group are more susceptible to changes than nodes in the smaller group (for more details see the linear response theory [59]). In this manner, additional cross-links exert a more pronounced impact on the larger group than on the smaller group.

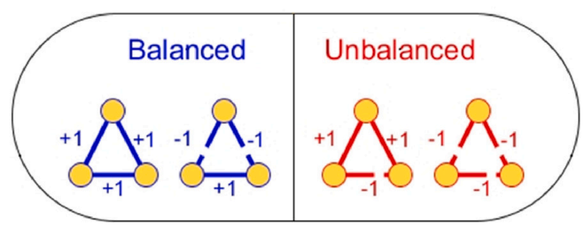

Fig. 8. Balanced and unbalanced triads (in the strong sense). The symbol $+1$ represents a positive polarization of a link between two agents (indicating friendship), while -1 denotes a negative link polarization (indicating enmity).

This model can complement the study of the structure of political blogs in the two months preceding the U.S. Presidential Election of 2004 [60], which demonstrated that liberal and conservative blogs form loosely connected echo chambers. Notably, conservative blogs are more frequently interlinked, creating a denser pattern. A similar observation regarding differing connection densities was noted in conservative and liberal Twitter communities in the U.S. in 2009 [61] and this distinction correlated with higher homophily among conservative Twitter users. It can be speculated that conservative voters in the U.S. generally form denser clusters, which are inherently more stable than liberal communities. Such characteristics can play a significant role in influencing the outcomes of successive elections.

4. Three-body interactions: when a friend of my enemy is my enemy

The models described in the previous sections assumed binary interactions between agents. Now, I will consider interactions related to the

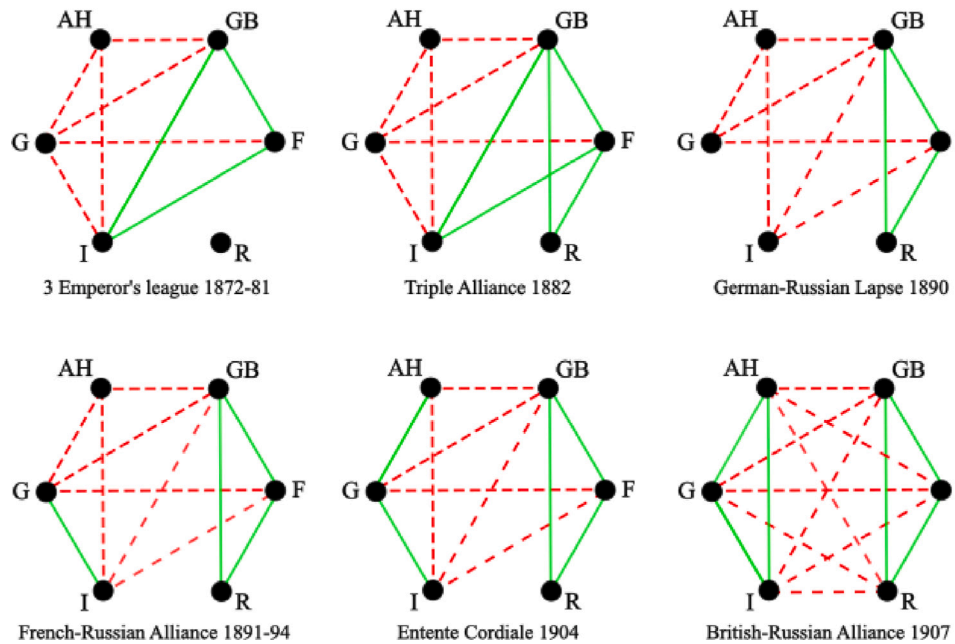

Fig. 9. Evolution of treaties between France (F), Great Britain (GB), Austria–Hungary (AH), Germany (G), Italy (I), and Russia (R) during the late 19th and early 20th centuries, leading to the formation of a structural balance — a division into two hostile coalitions [35]. Full green lines represent friendship relations, while dashed red lines represent enmity relations.

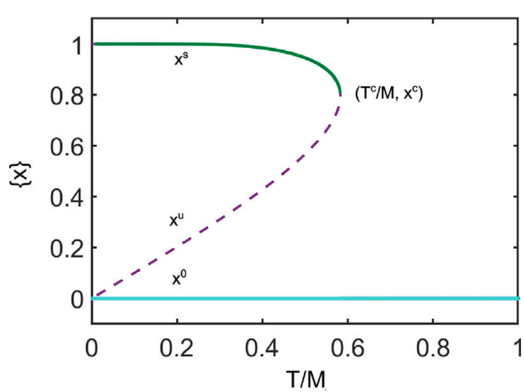

Fig. 10. Mean values of link polarizations for Heider balance in the full graph [36]. At the point $T^c/M = 1/a^c \approx 0.583\cdots$ ($x^c \approx 0.796\cdots$), a discontinuous transition occurs between the upper branch x^s and the solution $x^0 = 0$. The branch x^u serves as a separatrix between domains of attraction for the two stable solutions, for details see [36].

so-called Heider structural balance [32–35,62–65]. These interactions involve triple interactions and correspond to the following rules:

(a) A friend of my friend is my friend.
(b) A friend of my enemy is my enemy.
(c) An enemy of my friend is my enemy.
(d) An enemy of my enemy is my friend.

If all four rules are obeyed, then a corresponding triad is said to be in a state of *strong structural balance*. If only rules 1, 2, and 3 are obeyed, then it is referred to as *weak structural balance*. In this discussion, we will focus on systems driven by strong structural balance. Fig. 8 illustrates balanced and unbalanced triads (in the strong sense) using polarizations of links between agents.

For a complete graph of interacting agents, a structural balance implies that all link polarizations are positive, forming a state of *paradise*, or the system consists of two mutually antagonistic but internally friendly cliques. Fig. 9 illustrates changes in European treaties during the late 19th and early 20th centuries [35] where green links represent friendship relations and dashed red links represent enmity relations. The first important treaty was *3 Emperors League* in the period 1872–81. Next treaties, which are shown on these graphs reveal that finally two groups of states emerged: Great Britain, France and Russia had formed one group with friendship treaties, similarly Austria-Hungary, Germany and Italy had formed a second group with friendship treaties but between both groups only negative relations existed.

The division into two hostile coalitions is considered to be one of the contributing factors to the outbreak of the First World War. According to [25] … *the war came in 1914 because then, for the first time, the lines were sharply drawn between the two rival groups, and neither could yield on the Serbian issue without seeing the balance pass definitely to the other side*.

Consider a complete graph with N agents labelled by the index $i = 1, 2, 3, \dots, N$. The polarization of a link between nodes i and j is denoted as a dynamical variable $x_{ij}(t) = \pm 1$. From Fig. 8, it follows that a triad (i, j, k) is balanced only if the product of all three polarizations is equal to 1, i.e., $x_{ij}x_{jk}x_{ki} = 1$. The dynamics toward Heider balance can be expressed as follows:

$$x_{ij}(t+1) = \mathrm{sign}(B_{ij}(t)), \tag{10}$$

$$B_{ij}(t) = \sum_{k}^{M_{ij}} x_{ik}(t)x_{kj}(t), \tag{11}$$

where the summation in Eq. (11) goes through M_{ij} common nearest neighbours of connected nodes i and j. The sum $B_{ij}(t)$ can be considered a local field acting on the link x_{ij} (similarly as the social impact I_i in the SIT model given by Eq. (2)), and this dynamic behaviour is part of complex contested contagion [37]. The field B_{ij} can be derived from the Hamiltonian [34]:

$$\mathcal{H} = -\sum_{i>j>k}^{N} x_{ij}x_{jk}x_{ki}. \tag{12}$$

This Hamiltonian implies that the system can lower its energy if the product of link polarizations $x_{ij}x_{jk}x_{ki}$ in a triangle ijk is positive, aligning with the assumptions of strong structural balance. The deterministic social balance dynamics (10) can be extended by introducing a social

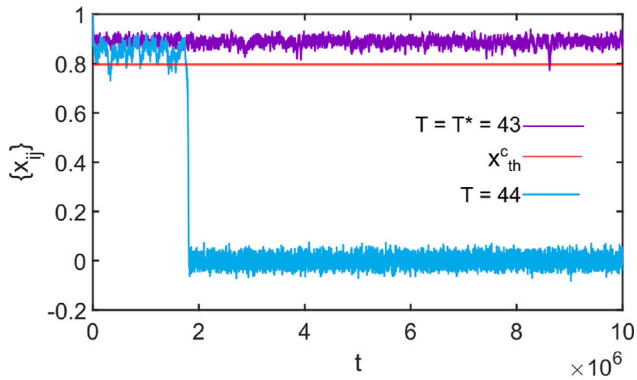

Fig. 11. Time evolution (Monte Carlo dynamics) of mean link polarization x_{ij} for a model of structural balance in a complete graph of size $N = 80$ at two different temperatures. For $T = 43$, a non-zero link polarization was observed over ten millions time steps. For $T = 44$, a transition to a disordered state occurred after two millions time steps. The mean-field critical temperature derived from Eq. (13) is $T^c = 45.5$, for details see [36].

temperature T, similar to the Glauber dynamics for Ising-like models discussed earlier. In the mean-field approximation [36], the mean link polarization can be determined as a fixed point of the equation:

$$x(t+1) = \tanh[ax^2(t)], \tag{13}$$

where $a = M/T$, and $M = N-2$ represents the number of different triangles containing a given edge ij. For any positive value of the parameter a, Eq. (13) possesses a stable fixed point $x^0 = 0$. When $a > a^c \approx 1.716$, another stable fixed point x^s emerges, depicted as the upper branch in Fig. 10. This solution implies that below a critical temperature $T^c \approx 0.583M$ (when the noise in the system is sufficiently small), a phase characterized by predominantly positive links, resembling the paradise state, can exist. However, as the temperature surpasses T^c, a discontinuous transition occurs, leading to a disordered phase with mean link polarization equal to $x = 0$. In this phase, the number of positive and negative links is the same. The abrupt change in mean link polarization has been verified through Monte Carlo simulations [36], as shown in Fig. 11.

Since the stable solution $x^0 = 0$ holds true for any temperature, observing the close-to-paradise solution x^s is not feasible when the temperature is high and subsequently reduced below T^c. This is because the temperature T^c is the tipping point of our system. In other words, the system exhibits hysteresis behaviour, making it impossible to return to the paradise state after departing from it. A thorough analysis [36] indicates that as the temperature decreases, the system enters a phase marked by two cliques of similar sizes, characterized by exclusively positive internal links. However, all links between these cliques are negative. This phase corresponds to the network of international relations in Europe following the British–Russian Alliance of 1907, as depicted in the bottom right graph of Fig. 9.

Let us observe the existence of multiple equilibria within this system, similar to what was discussed for the models of the strong leader and weakly coupled communities. One equilibrium is the "paradise" state, which can only occur under low noise levels. Eq. (13), however, possesses a second solution $x^0 = 0$ that is consistently present and corresponds to a state of two cliques for low noise levels. In fact, there are numerous possibilities to form such cliques, whereas only one paradise state can exist. Once the stability of the paradise state is compromised, the probability of the system reverting to this state when noise levels decrease becomes exceedingly low.

5. Conclusions

The exploration of three distinct systems describing collective social behaviour — namely, the social impact model with a strong leader, weakly coupled communities with Ising dynamics, and a complete graph with triadic interactions illustrating structural balance — has revealed a commonality: all of these systems exhibit discontinuous transitions. These transitions manifest as the sudden disappearance of opposition with the leader's strength or noise magnitude reaching a critical value, the abrupt change of the entire community's opinion with the interlink count to another community hitting a critical value, and the sudden reduction in the number of positively polarized links beyond a critical temperature. Notably, these transitions are irreversible, characterized by hysteresis behaviour that resists the restoration of prior states even after altering parameters.

The transitions discussed correspond to tipping points, specifically the so-called *fold catastrophes* [66], which are observed in various systems, including the majority model of a network with communities [55] and an activity-driven temporal bilayer echo-chamber system [67].

In response to the central question posed in this paper — why history surprises us — these nonlinear collective dynamics that drive social evolution indeed yield surprising results. Traditional expectations of smooth, reversible changes in social structures are challenged, as certain cases reveal catastrophic, irreversible transitions. These transitions, arising at tipping points in multistable systems, underscore the difficulty of reversing changes once a parameter or collective observable crosses a critical threshold.

Declaration of competing interest

The authors declare that they have no known competing financial interests or personal relationships that could have appeared to influence the work reported in this paper.

Data availability

Data will be made available on request.

Declaration of Generative AI and AI-assisted technologies in the writing process

During the preparation of this work the author used Chat GPT 3.5 in order to improve language and readability. After using this tool/service, the author reviewed and edited the content as needed and take full responsibility for the content of the publication.

Acknowledgements

I would like to express my gratitude to numerous individuals with whom I have collaborated on the models discussed therein. I am thankful to Piotr Fronczak and Łukasz Gajewski for developing codes enabling computer simulations, to Krzysztof Kacperski and Krzysztof Malarz for their agreement to use figures from our papers and to Patryk Bojarski, Piotr Górski and Mohandas Krishnadas for their assistance in editing this manuscript. This research has received funding from the Polish National Science Center, grant Alphorn No. 2019/01/Y/ST2/00058.

References

[1] Wolfgang Weidlich, Synergetic modelling concepts for sociodynamics with application to collective political opinion formation, J. Math. Sociol. 18 (4) (1994) 267–291.
[2] Wolfgang Weidlich, Sociodynamics applied to the evolution of urban and regional structures, Discrete Dyn. Nat. Soc. 1 (2) (1997) 85–98.
[3] Wolfgang Weidlich, Sociodynamics—-a systematic approach to mathematical modelling in the social sciences, Chaos Solitons Fractals 18 (3) (2003) 431–437.
[4] J.A. Hołyst, K. Kacperski, F. Schweitzer, Social impact models of opinion dynamics, Annual Rev. Comput. Phys. IX (2001) 253–273.
[5] Philip Ball, The physical modelling of society: a historical perspective, Physica A 314 (1–4) (2002) 1–14.

[6] C.M. Bordogna, E.V. Albano, Statistical methods applied to the study of opinion formation models: a brief overview and results of a numerical study of a model based on the social impact theory, J. Phys. Conden. Matter 19 (6) (2007) 065144.
[7] Claudio Castellano, Santo Fortunato, Vittorio Loreto, Statistical physics of social dynamics, Rev. Modern Phys. 81 (2) (2009) 591–646, PT: J; UT: WOS:000267197500005.
[8] Dietrich Stauffer, A biased review of sociophysics, J. Stat. Phys. 151 (1) (2013) 9–20.
[9] Parongama Sen, Bikas K. Chakrabarti, Sociophysics: An Introduction, Oxford University Press, 2014.
[10] Serge Galam, Sociophysics: A Physicist's Modeling of Psycho-Political Phenomena, Springer, 2016.
[11] Marko Jusup, Petter Holme, Kiyoshi Kanazawa, Misako Takayasu, Ivan Romić, Zhen Wang, Sunčana Geček, Tomislav Lipić, Boris Podobnik, Lin Wang, et al., Social physics, Phys. Rep. 948 (2022) 1–148.
[12] David Lazer, Alex Pentland, Lada Adamic, Sinan Aral, Albert-Laszlo Barabasi, Devon Brewer, Nicholas Christakis, Noshir Contractor, James Fowler, Myron Gutmann, Tony Jebara, Gary King, Michael Macy, Deb Roy, Marshall Van Alstyne, Social science Computational social science, Science 323 (5915) (2009) 721—723.
[13] Frank Schweitzer, Sociophysics, Physics Today 71 (2) (2018) 40–46.
[14] Jun Zhang, Wei Wang, Feng Xia, Yu-Ru Lin, Hanghang Tong, Data-driven computational social science: A survey, Big Data Res. 21 (2020) 100145.
[15] Michael W. Macy, Manqing Ma, Daniel R. Tabin, Jianxi Gao, Boleslaw K. Szymanski, Polarization and tipping points, Proc. Natl. Acad. Sci. 118 (50) (2021) e2102144118.
[16] Katarzyna Sznajd-Weron, Józef Sznajd, Tomasz Weron, A review on the sznajd model—20 years after, Physica A 565 (2021) 125537.
[17] Dirk Helbing, Peter Molnar, Social force model for pedestrian dynamics, Phys. Rev. E 51 (5) (1995) 4282.
[18] Dirk Helbing, Traffic and related self-driven many-particle systems, Rev. Modern Phys. 73 (4) (2001) 1067.
[19] Debashish Chowdhury, Ludger Santen, Andreas Schadschneider, Statistical physics of vehicular traffic and some related systems, Phys. Rep. 329 (4–6) (2000) 199–329.
[20] Marc Barthelemy, The statistical physics of cities, Nat. Rev. Phys. 1 (6) (2019) 406–415.
[21] Matjaž Perc, Jillian J. Jordan, David G. Rand, Zhen Wang, Stefano Boccaletti, Attila Szolnoki, Statistical physics of human cooperation, Phys. Rep. 687 (2017) 1–51.
[22] Peter Richmond, Bertrand M. Roehner, Ali Irannezhad, Stefan Hutzler, Mortality: A physics perspective, Physica A 566 (2021) 125660.
[23] Santo Fortunato, Carl T. Bergstrom, Katy Börner, James A. Evans, Dirk Helbing, Staša Milojević, Alexander M. Petersen, Filippo Radicchi, Roberta Sinatra, Brian Uzzi, et al., Science of science, Science 359 (6379) (2018) eaao0185.
[24] Michael I. Handel, Surprise and change in international politics, Int. Secur. 4 (4) (1980) 57–85.
[25] Bernadotte E. Schmitt, Triple alliance and triple entente, 1902–1914, Am. Histor. Rev. 29 (3) (1924) 449–473.
[26] Ian Kershaw, Hitler, Routledge, 2014.
[27] Egbert H. Van Nes, Babak M.S. Arani, Arie Staal, Bregje van der Bolt, Bernardo M. Flores, Sebastian Bathiany, Marten Scheffer, What do you mean,'tipping point'? Trends Ecol. Evol. 31 (12) (2016) 902–904.
[28] Simon A. Levin, Helen V. Milner, Charles Perrings, The dynamics of political polarization, Proc. Natl. Acad. Sci. 118 (50) (2021) e2116950118.
[29] Casper van Elteren, Rick Quax, Peter Sloot, An information theory perspective on tipping points in dynamical networks, 2022, arXiv preprint arXiv:2207.14016.
[30] K. Kacperski, J.A. Hołyst, Phase transitions and hysteresis in a cellular automata-based model of opinion formation, J. Stat. Phys. 84 (1996) 169–189.
[31] Janusz A. Hołyst, Krzysztof Kacperski, Frank Schweitzer, Phase transitions in social impact models of opinion formation, Physica A 285 (1) (2000) 199–210.
[32] F. Heider, Attitudes and cognitive organization, J. Psychol. 21 (1) (1946) 107–112.
[33] Elliot Aronson, Vernon Cope, My enemy's enemy is my friend, J. Personal. Soc. Psychol. 8 (1p1) (1968) 8.
[34] Tibor Antal, Paul L. Krapivsky, Sidney Redner, Dynamics of social balance on networks, Phys. Rev. E 72 (3) (2005) 036121.
[35] Tibor Antal, Paul L. Krapivsky, Sidney Redner, Social balance on networks: The dynamics of friendship and enmity, Physica D 224 (1) (2006) 130–136.
[36] Krzysztof Malarz, Janusz A. Hołyst, Mean-field approximation for structural balance dynamics in heat-bath, 2019, http://dx.doi.org/10.48550/ARXIV.1911.13048.
[37] Damon Centola, Michael Macy, Complex contagions and the weakness of long ties, Am. J. Sociol. 113 (3) (2007) 702–734.
[38] Bibb Latané, The psychology of social impact., Am. Psychol. 36 (4) (1981) 343.
[39] Bibb Latané, Sharon Wolf, The social impact of majorities and minorities., Psychol. Rev. 88 (5) (1981) 438.
[40] Maciej Lewenstein, Andrzej Nowak, Bibb Latané, Statistical mechanics of social impact, Phys. Rev. A 45 (2) (1992) 763.
[41] Robert B. Cialdini, Carl A. Kallgren, Raymond R. Reno, A focus theory of normative conduct: A theoretical refinement and reevaluation of the role of norms in human behavior, in: Advances in Experimental Social Psychology, Vol. 24, Elsevier, 1991, pp. 201–234.
[42] Bibb Latané, Martin J. Bourgeois, Experimental evidence for dynamic social impact: The emergence of subcultures in electronic groups, J. Commun. (1996).
[43] Rodrigo Perez-Vega, Kathryn Waite, Kevin O'Gorman, Social impact theory: An examination of how immediacy operates as an influence upon social media interaction in facebook fan pages, Mark. Rev. 16 (3) (2016) 299–321.
[44] Krzysztof Kacperski, Janusz A. Hołyst, Phase transitions as a persistent feature of groups with leaders in models of opinion formation, Physica A 287 (3) (2000) 631–643.
[45] W. Lance Bennett, White noise: The perils of mass mediated democracy, Commun. Monographs 59 (4) (1992) 401–406.
[46] Maxwell T. Boykoff, S. Ravi Rajan, Signals and noise: Mass-media coverage of climate change in the USA and the UK, EMBO Rep. 8 (3) (2007) 207–211.
[47] Kalina Christoff, Alan Gordon, Rachelle Smith, B.C. Vancouver, The role of spontaneous thought in human cognition, Neurosci. Decis. Making 1 (2011) 259–284.
[48] Martin Lages, Katarzyna Jaworska, How predictable are "spontaneous decisions" and "hidden intentions"? Comparing classification results based on previous responses with multivariate pattern analysis of fMRI BOLD signals, Front. Psychol. 3 (2012) 56.
[49] Dirk Helbing, Illés J. Farkas, Tamás Vicsek, Freezing by heating in a driven mesoscopic system, Phys. Rev. Lett. 84 (2000) 1240–1243.
[50] Historical Exhibition Presented by The German Bundestag, Elections in the Weimar Republic, 2023, http://web.archive.org/web/20080207010024/http://www.808multimedia.com/winnt/kernel.htm. (Accessed 21 August 2023).
[51] Wikipedia, Nazi Party, 2023, https://en.wikipedia.org/wiki/Nazi_Party. (Accessed 21 August 2023).
[52] Jürgen W. Falter, Thomas Lindenberger, Siegfried Schumann, Dirk Hänisch, Wahlen und Abstimmungen in der Weimarer Republik: Materialien zum Wahlverhalten 1919–1933, Beck, 1986.
[53] Alfred Milatz, Wähler und Wahlen in der Weimarer Republik, 1965.
[54] Michelle Girvan, Mark E.J. Newman, Community structure in social and biological networks, Proc. Natl. Acad. Sci. 99 (12) (2002) 7821–7826.
[55] R. Lambiotte, M. Ausloos, J.A. Hołyst, Majority model on a network with communities, Phys. Rev. E 75 (2007) 030101.
[56] Andrea Lancichinetti, Santo Fortunato, Community detection algorithms: a comparative analysis, Phys. Rev. E 80 (5) (2009) 056117.
[57] K. Suchecki, J.A. Hołyst, Ising model on two connected Barabasi–Albert networks, Phys. Rev. E 74 (2006) 011122.
[58] K. Suchecki, J.A. Hołyst, Bistable-monostable transition in the ising model on two connected complex networks, Phys. Rev. E 80 (2009) 031110.
[59] James J. Binney, Nigel J. Dowrick, Andrew J. Fisher, Mark E.J. Newman, The Theory of Critical Phenomena: an Introduction to the Renormalization Group, Oxford University Press, 1992.
[60] Lada A. Adamic, Natalie Glance, The political blogosphere and the 2004 US election: divided they blog, in: Proceedings of the 3rd International Workshop on Link Discovery, 2005, pp. 36–43.
[61] Andrei Boutyline, Robb Willer, The social structure of political echo chambers: Variation in ideological homophily in online networks, Political Psychol. 38 (3) (2017) 551–569.
[62] Leon Festinger, A Theory of Cognitive Dissonance, Stanford University Press, 1957.
[63] F. Harary, On the measurement of structural balance, Behav. Sci. 4 (4) (1959) 316–323.
[64] M.J. Krawczyk, K. Kułakowski, Structural balance of opinions, Entropy 23 (11) (2021) 1418.
[65] Piotr J. Górski, Klavdiya Bochenina, Janusz A. Hołyst, Raissa M. D'Souza, Homophily based on few attributes can impede structural balance, Phys. Rev. Lett. 125 (7) (2020) 078302.
[66] Marten Scheffer, Jordi Bascompte, William A. Brock, Victor Brovkin, Stephen R. Carpenter, Vasilis Dakos, Hermann Held, Egbert H. Van Nes, Max Rietkerk, George Sugihara, Early-warning signals for critical transitions, Nature 461 (7260) (2009) 53–59.
[67] Ł.G. Gajewski, J. Sienkiewicz, J.A. Hołyst, Transitions between polarization and radicalization in a temporal bilayer echo-chamber model, Phys. Rev. E 105 (2022) 024125.

Janusz A. Hołyst is a Professor at Faculty of Physics, Warsaw University of Technology where he leads the Group of Physics in Economy and Social Sciences. He is one of the pioneers in using methods of physics to model economic and social processes. His current research includes simulations of evolving networks, models of collective opinion and emotion formation, econophysics, statistical physics, and data science. He has supervised 16 completed PhD thesis and published around 170 papers (according to Google Scholar over 6700 citations, h=41). He collaborates with Institutes in Austria, Germany, Israel, Japan, Netherlands, UK, Switzerland, Slovenia, Singapore and USA, where he spent over 7 years as a Visiting Professor or Guest Scientist. He is a Main Editor of Physica A, Assoc. Editor of Journal of Comput. Science and a former Editor of European Physical Journal B and of EPJ Data Science. He was a coordinator/partner in several EU Projects, e.g. *Collective Emotions in Cyberspace* or *Reverse Engineering of Social Information Processing*. Currently he coordinates the EU Project OMINO – Overcoming Multilevel Information Overload, http://www.ominoproject.eu He is the President of *KRAB* - the Polish *National Council of EU Research Projects Coordinators* and a former Chairman of *FENS - Physics in Economy and Social Sciences*, Division of the *Polish Physical Society*. In 2021, he was nominated for the *Marian Smoluchowski Medal* of *Polish Physical Society*
Web page: http://if.pw.edu.pl/~jholyst/
Google scholar: https://scholar.google.com/citations?hl=pl&user=KA_kg0IAAAAJ